10th International Conference on
Particle Induced X-ray Emission and its Analytical Applications
PIXE 2004, Portorož, Slovenia, June 4-8, 2004
http://pixe2004.ijs.si/

The role of metallic impurities in the interaction of carbon nanotubes with microwave radiation

F. Naab, M. Dhoubhadel, O.W. Holland, J.L. Duggan, J. Roberts and F.D. McDaniel

Department of Physics, P.O. Box 311427, University of North Texas, Denton, TX 76203-1427, USA

ABSTRACT

Microwave interaction with single-walled, carbon nanotubes (SWNTs) in vacuum has been shown to result in rather dramatic effects including highly ionized plasmas, high temperatures, and unique morphological changes. The mechanism for absorption of microwave energy in SWNTs is contested and centers on the role of metallic impurities. Such impurities, especially Fe, are introduced during the synthesis process as a catalyst to control the morphology of the SWNTs. In this work, the absorption of microwave energy was determined for different types of carbon nanotubes, including multi-walled and double-walled varieties. Particle Induced X-Ray Emission (PIXE) analysis was done to identify the impurities and their concentrations in the samples. Also, low-temperature gas desorption from the carbon nanotubes was studied. The results indicate that metallic impurities do not play an important role in the absorption of microwave energy by carbon nanotubes but rather structural properties dominate.

Keywords: thick samples; PIXE; carbon nanotubes; impurities; microwave radiation.

1. INTRODUCTION

The interaction of microwave radiation with matter is of fundamental and technological importance. Microwave technology is widely utilized in the food industry for heating, sterilization, drying, freeze-drying, etc., and in chemical processing [1] where it provides better control of temperature/pressure during synthesis. Recently, microwave heating of graphite to produce carbon nanotubes (CNTs) has been demonstrated [2]. A nanotube is an allotrope of carbon with unique electronic and mechanical properties derived from its Fullerene structure.* Microwaves offer advantages over standard thermal methods that can be integrated into many CNTs applications where thermal activation is required.

Recently, studies have been done to understand the microwave absorption by single-wall carbon nanotubes (SWNTs) with conflicting results. The formation of SWNTs involves the use of metallic catalyst such as Fe, Ni, Co, etc. to promote the formation of SWNTs over other varieties of nanotubes, i.e. multi-walled (MWNTs) and double-walled nanotubes (DWNTs). Thus, carbon nanotubes are inherently not pure and contain a host of metallic impurities as well as other forms of carbon such as polyhedral particles and amorphous carbon. One study [3] compared the behavior of raw and purified SWNTs and concluded that microwave energy is predominantly absorbed as a result of a magnetic resonance within the ferromagnetic Fe catalyst particles. Another study reported no differences in the behavior of raw and purified SWNTs in a microwave field [4]. However, both studies suffered from a common problem. CNTs have a propensity to adsorb gases [5]. In both studies, gas desorption during microwave irradiation initiated an extremely hot plasma contiguous to the SWNTs sample. Since the plasma strongly couples with the microwave radiation, it provides an independent mechanism for absorbing microwave energy. While this coupling will depend upon the amount and rate of gas desorption from the sample, it will not be affected by metallic impurities. Also, the hot plasma can conductively couple to the sample to cause a substantial rise in temperature.

The interaction of various types of CNTs (i.e. SWNTs, DWNTS, and MWNTs) with 2.45 GHz microwaves from a 600 W source in high vacuum (~10^{-6} torr) conditions is reported in this paper. A variety of other materials including powdered graphite were investigated for comparison to the CNTs. Prior to irradiation, all the samples were degassed to suppress plasma formation during microwave exposure. Particle-Induced X-ray Emission (PIXE) analysis was done to identify impurities and their

* http://en.wikipedia.org/wiki/Carbon_nanotube

concentration in the carbon samples. A residual gas analyzer (RGA) was used to monitor the released gases, e.g. H_2, during the degassing process. While differences in the microwave absorption were observed between the various types of nanotubes, the differences could not be correlated with impurities in the samples. Rather, a correlation was found between the microwave interaction and thermally activated release of H_2 in the different types of CNTs.

2. PIXE ANALYSIS

Samples were irradiated with 1.5 MeV protons using a 2.5 MV Van de Graaff accelerator at the University of North Texas. The HPGe X-ray detector was positioned at a backscattering angle $\theta = 145°$ and the beam's incident angle on the sample was $\alpha = 17°$ (see figure 1). The samples were biased at +300 V for efficient collection of secondary electrons for current integration.

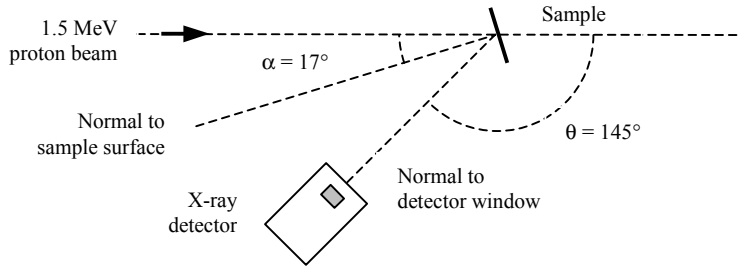

FIGURE 1. Sketch of the experimental setup.

The CNTs samples were in two forms: powder and small balls of ~1 mm in diameter. The samples were mounted between two plastic foils attached to a supporting metal frame; an 8.5-μm thick Kapton foil on the backside and a 0.15-μm AP1 Moxtek film on the front. The Moxtek film is thin enough to avoid corrections due to beam energy loss and X-ray attenuation. The aluminum frame was covered with carbon tape to avoid X-ray production in the frame due to the scattered beam. Secondary X-ray fluorescence in the aluminum frame was completely negligible.

The efficiency of the X-ray detector was determined for eighteen Kα transitions of different elements using thin targets [6]. A polynomial fit was done using *lspline* and *interp* functions of Mathcad 8.0 to the natural logarithm of the experimental values.

The calculation of the mass concentration for each element was done using the following expression corresponding to a thick sample:

$$C_Z = \frac{N_X \, A_Z}{\varepsilon_Z \, b_Z \, N_p \int_{E_0}^{0} \frac{\sigma_Z(E) T_Z(E)}{S_M(E)} \, dE} \qquad (1)$$

where N_X is the number of counts of the Kα or Lα transition in the X-ray spectrum, A_Z is the atomic mass of the element, ε_Z is the detector's absolute efficiency (which includes detector's intrinsic efficiency and solid angle) for the Kα or Lα transition, b_Z is the intensity fraction of the Kα or Lα transition [7], N_p is the number of particles that interact with the target during the spectrum acquisition, σ_Z is the elemental K-shell or L-shell X-ray production cross section, T_Z is the transmission in the sample of the Kα or Lα X-ray in its way towards the detector from the point where they are produced and S_M is the stopping power of the matrix of the sample. The AXIL code [8] was used to fit the spectra. We assumed the matrix of the sample to be 100 % carbon. The mass attenuation coefficients were obtained from Ref. [9]. Discrete values for σ_Z and S_M were obtained from ISICS code [10] and SRIM code [11]; respectively. A polynomial function was fitted to each of these sets of values to evaluate Eq. (1) using the Mathcad code.

3. RESULTS

Table 1 lists the nanotube materials analyzed using PIXE and some of their characteristics. Figure 2a shows the PIXE for the SWNTs used in this study. The results show that all the SWNTs (independent

of vendor and average size) contain large amounts (~ 9 % or less) of metallic impurities. Elemental variations among the various types of SWNTS are mainly due to the different catalyst material used by the vendors during growth. Despite these variations, the total amount of metallic impurities, given in the rightmost portion of the figure, is nearly the same in all the SWNTs samples. Figure 2b gives the impurity concentrations in the different types of nanotubes, as well as graphite. Significant differences are observed in these samples. It is clear that both SWNTs and DWNTs contain substantially more metallic impurities than either MWNTs or graphite.

Material	I.D. [nm]	O.D. (Avg.) [nm]	Length [μm]	Temperature [K]
Single Wall[1]		0.8-2 (1.1)	0.5-100	~3000
Buckypearls (SW)[2]		1-1.5		
Double Wall[1]	1.3-2.0	<5	0.5-50	~1900
Multi Wall[1]	5-10	60-100	0.5-50	~3000
Graphite				~1700
P-type Silicon				~1400

TABLE 1. List of nanotubes materials analyzed using PIXE and exposed to microwave radiation.
[1] Vendor: Nanostructured & Amorphous Materials, Inc.
[2] Carbon Nanotechnologies, Inc.

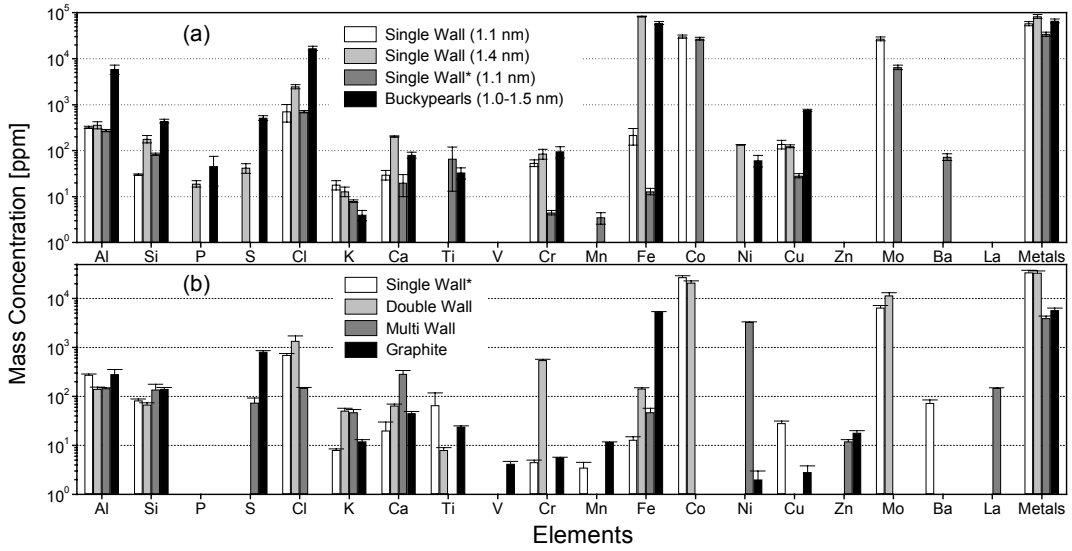

FIGURE 2. Mass Concentration for those elements found in different carbon nanotube materials. Also, impurities in graphite are shown for comparison.

An Ocean Optics Spectrometer with a charge coupled device detector sensitive over a wavelength range of 300-900 nm was used to acquire emission spectra from the CNTs during microwave exposure. The spectrometer was set to a continuous acquire mode so that the temperature profile of the samples during the entire exposure could be determined (from the blackbody radiation). Samples other than CNTs spanning a wide range in electrical resistivity were used to establish an Ohmic response, i.e. heating caused by induced currents through electrical (Ohmic) resistance. Figure 3 compares the resistivity of these samples to the maximum temperature achieved during microwave exposure. It is clear that the results intersect a smooth response curve indicating a normal retrograde behavior, i.e. small net absorption at both ends due to transmission for insulators and high reflectance for highly conductive metals. Net absorption is expected to peak for some intermediate value of resistivity as is observed. The result for the DWNTs (1800 K) is consistent with this trend and is nearly identical to that from graphite.

However, the results (~3000 K) for both the SWNTs and MWNTS are anomalous and not easily interpreted in terms of only Ohmic heating. When compared with the PIXE results, there is no correlation between total metallic impurities and microwave absorption. Therefore, it is concluded that such impurities do not play a dominant role in this process.

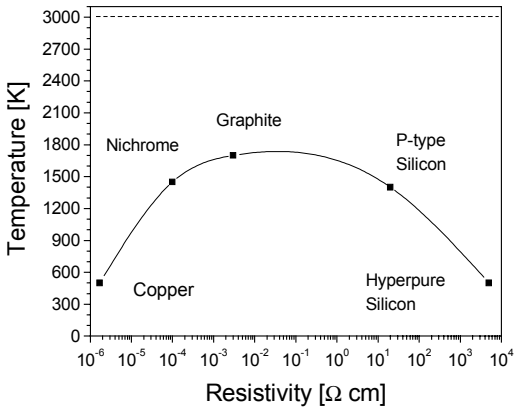

FIGURE 3. Qualitative behavior of the maximum temperature reached by different materials as a function of their resistivity at room temperature when exposed to microwave radiation in a high vacuum system (~10^{-6} torr). The optical spectrometer is sensitive to temperatures greater than ~1000 K. Approximate values were placed on the plot for Cu and hyperpure Si. The dashed line at 3000 K suggests the temperatures reached by SWNT and MWNT samples, since their resistivities are unknown.

Desorption measurements provided some indication that structural differences may be responsible. Of the three types of CNTs, only DWNTs exhibited an observable release of hydrogen during degassing to ~ 400 ºC. This behavior mimics the trend seen in the microwave experiments, i.e. the DWNTs behave differently than either SWNTs or MWNTs.

4. CONCLUSIONS

Differences were observed in CNTs when irradiated by microwaves. While Ohmic behavior during exposure is sufficient to account for the temperature rise in the DWNTs, the results for both SWNTs and MWNTs are more complicated. They suggest another heating mechanism is operative in these samples. While this analysis ignores any differences in emissivity, large variations are not expected between CNTs. No correlation was established between the microwave effects and impurities in the samples indicating that impurities do not play a substantial role in the heating process. Structural differences may account for both the gas desorption and microwave results.

ACKNOWLEDGEMENTS

Work at UNT supported in part by NSF, ONR, Texas Advanced Technology Program, and the Robert A. Welch Foundation.

REFERENCES

1. Kharissova O.V., Ortiz U. and Hinojosa M., Mat. Res. Soc. 654 AA.3.14.1 (2001).
2. Varadan V.K. and Xie J., Smart Mater. Struct. 11, 610 (2002).
3. Wadhawan A., Garrett D., and Perez J.M., Appl. Phys. Lett. 83, 2683-2685 (2003).
4. Imholt T.J., Dyke C.A., Hasslacher B., Perez J.M., Price D.W., Roberts J.A., Scott J.B., Wadhawan A., Ye Z. and Tour J.M., Chem. Matter. 15, 3969-1970 (2003).
5. Ding R.G., Liu G.Q., Yan Z.F. and Wilson M.A., J. of Nanoscience and Nanotechnology 1, 7 (2000).
6. Lennard W.N. and Phillips D., Nucl. Instr. and Meth. 166, 521-529 (1979).
7. Table of Isotopes, edited by Firestone R.B. and Shirley V.S., New York: John Wiley & Sons, 1996.
8. Van Espen P., Nullens H. and Adams F., Nucl. Instr. and Meth. 142, 243-250 (1977).
9. Orlic I., Loh K.K., Sow C.H., Tang S.M. and Thong P., Nucl. Instr. and Meth. B74, 352-361 (1993).
10. Liu Z. and Cipolla S.J., Computer Physics Communications 97, 315-330 (1996).
11. Ziegler J.F., Biersack J.P., Littmark U., The Stopping and Range of Ions in Solids, New York: Pergamon, 1999.